

A method for sparse and robust independent component analysis

Lauri Heinsonen^{a,*}, Joni Virta^a

^a*Department of Mathematics and Statistics, University of Turku, 20014 Turku, Finland*

Abstract

This work presents sparse invariant coordinate analysis, SICS, a new method for sparse and robust independent component analysis. SICS is based on classical invariant coordinate analysis, which is presented in such a form that a LASSO-type penalty can be applied to promote sparsity. Robustness is achieved by using robust scatter matrices. In the first part of the paper, the background and building blocks: scatter matrices, measures of robustness, ICS and independent component analysis, are carefully introduced. Then the proposed new method and its algorithm are derived and presented. This part also includes a consistency result for a general case of sparse ICS-like methods. The performance of SICS in identifying sparse independent component loadings is investigated with simulations. The method is also illustrated with example in constructing sparse causal graphs.

Keywords:

independent component analysis, invariant coordinate selection, LASSO, robustness, scatter matrix, sparsity
 2020 MSC: Primary 62H25, Secondary 62F35, 62J07

1. Introduction

A common goal in statistics and data science is to break down the variation in data to some factors. In this article this problem is tackled with sparse independent component analysis where the variables in data are decomposed into a linear combination of independent latent components (sources). The components are built so that only a subset of the original variables are linked to a particular component (sparsity).

In independent component analysis (ICA) the observed random vector x is assumed to be an unknown deterministic mix of unknown random and independent sources [25]. This (basic linear) independent component model can be written as

$$x = \mu + \Omega z,$$

where x is the observed vector, μ some deterministic mean, Ω is the mixing matrix and z is the source vector with independent components. The objective of ICA is to, given a random sample x_1, \dots, x_n from the model, find an unmixing matrix (estimate of Ω^{-1}) that can be used to obtain the values of the independent sources from the observations. Many different ICA methods have been proposed, for example JADE [6] and FastICA [24], see also the review in [34].

Our chosen way to solve the ICA problem comes from the invariant coordinate selection (ICS) [45]. In ICS, one has two scatter matrices S_1, S_2 , which are in certain sense generalizations of the covariance matrix. An example of such a matrix is the FOBI-matrix based on the fourth moments, see Section 2 for details. Now, one jointly diagonalizes the matrices by solving $S_2 v = \lambda S_1 v$. This procedure essentially first removes the variation measured by S_1 from the data and then finds a coordinate system (of which v is a basis vector) that maximizes the variation measured by S_2 . This way we can, in a sense, “compare” the variations measured by the scatter matrices, calculated on the same data, and get a new view on the data which best contrasts these two forms of variation, see [45] for examples. Several sub-cases of ICS have separate names and one example of such a method is classical ICA method FOBI [5], where

*Corresponding author. Email address: lauri.k.heinsonen@utu.fi

the scatter matrices are the covariance matrix and the FOBI-matrix. Also ICS with other scatter matrices can lead to the solution of the ICA problem and we discuss this relation closer in Section 2.

The purpose of this work is to develop, using ICS as a basis, a general methodology for sparse and robust independent component analysis, where by “robust” we mean that the method does not break down under the presence of outlying data points. Both topics have been separately pursued in the literature and we next review the most relevant works but, as far as we are aware, the combination of sparsity and robustness is entirely novel.

Independent component analysis and sparsity can be combined in two natural, but fundamentally different, ways. In *sparse component analysis*, the source vectors z are assumed to be sparse, see, e.g., [2, 4, 18, 30]. Sparse component analysis is at its most useful in specialized applications where we have reason to expect that a certain subset of the sources is “inactive” (taking only the value zero) at any given time. Whereas, in *sparse independent component analysis*, the unmixing matrix Ω^{-1} (or, sometimes, its inverse) is assumed to be sparse. In this work, we focus on this variant, sparse independent component analysis, due to its generality; the sparsity of Ω^{-1} leads to highly interpretable independent components, making the method a useful tool regardless of the application area.

Several non-robust sparse ICA methods have been proposed earlier in the literature, the most prevalent approach being formulating a likelihood function for the observations and using a sparsity-inducing penalty function: [26] took a Bayesian approach and formulated the penalization through conjugate priors, allowing fitting their model via standard ICA applied to an augmented sample; [47] used a SCAD-penalty in combination with post-estimation thresholding; [48] proposed using either adaptive LASSO or optimal brain surgeon, choosing their tuning parameters using AIC/BIC; [38] used directly a ℓ_0 -penalty; [9] used a combination of standard and group LASSO penalties; [20] used adaptive LASSO with a relaxed form of orthogonality; [33] maximize a constrained Gaussian likelihood under specific structural assumptions on Ω . Outside of likelihood-based approaches, [1] derived high-dimensional error bounds under a specific Gaussian form of ICA where the sparsity of Ω ensures the identifiability of the model, and [33] propose a second-order decomposition method for a specific class of structured mixing matrices Ω .

In this work, we take a different viewpoint from the above and implement sparsity using the framework in [29] that was inspired by the seminal LASSO-based sparse PCA method by [50]. While [29] focused exclusively on sparse sufficient dimension reduction, their framework is directly applicable to the scatter matrix formulation of ICA (and also ICS in general), a fact that appears not have been noticed earlier in the literature. Using this approach to achieve sparse and robust ICA is natural, as the robustness can be implemented to the procedure via the choice of scatter matrices, essentially separating the two aspects (sparsity and robustness) and allowing controlling them through individual tuning parameters.

Of earlier approaches to robust ICA, our work is most similar with [35] who likewise used robust scatter matrices to achieve robust estimation of independent components. Besides this, the previous literature on robust ICA includes maximizing robust measures of shape [3] or divergence [8], and using rank [28] and signed rank [19] based estimators to circumvent moment assumptions and to achieve semiparametric efficiency. None of the previous references allow for sparsity in the estimation of the independent components.

The main contributions and novelty in the current paper are the following:

- We propose a general framework of robust and sparse ICA. Unlike many of the previous works on sparse ICA [9, 20, 26, 38, 47, 48], our model is semiparametric (and not likelihood-based), meaning that we require neither the pre-specification nor the estimation of the densities of the latent sources. Moreover, both the level of sparsity and the level of robustness of the estimation are controlled via individual tuning parameters, making the method transparent and simple to use in practice.
- We establish the asymptotic convergence rate of the resulting estimator as a function of the convergence rates of the used scatter matrices. This result is not limited to ICA but actually applies to the joint diagonalization of any two scatter matrices. As such, it gives convergence rates also in the sufficient dimension reduction context [29] and in the fully general context of sparse ICS (SICS). Moreover, when compared to earlier works on asymptotics of sparse ICA [1, 9], our results do not make distributional assumptions and allow robustness.
- We extensively study the impact of sparsity and robustness on the finite-sample properties of the estimator using simulations. The results confirm that robust methods are needed when the data is contaminated and that sparse methods are clearly beneficial when the underlying situation is sparse. The results also suggest that the sparse and robust variants of the proposed method generally perform extremely well in the tested scenarios.

The paper is organized as follows. In Section 2 we review the concepts of a scatter matrix and independence property, and recall how they produce a solution to the ICA problem. Also several robust scatter matrices from the literature are presented. Section 3 sees us combining robust scatter matrices with the sparsity framework of [29] to obtain our proposed method. We also establish the convergence rate of the method in this section. In Section 4, we compare the performance of the method under different levels of sparsity and robustness using simulations, including also several competing methods in the evaluations. A real data example of estimating non-Gaussian causal graphs using sparse ICA is given in Section 5 and we conclude with discussion in Section 6.

2. Theoretical background

2.1. ICA solution using two scatter matrices

First let us define a location vector, a scatter matrix, the independence property and symmetrized scatter matrices.

Definition 1. Let $x \in \mathbb{R}^p$ be a random vector. A vector $T \in \mathbb{R}^p$, calculated from x , is a *location vector* if it is affine equivariant, in the sense that

$$T(Ax + b) = AT(x) + b$$

for all full rank matrices $A \in \mathbb{R}^{p \times p}$ and vectors $b \in \mathbb{R}^p$.

Definition 2. Let $x \in \mathbb{R}^p$ be a random vector. A matrix $S \in \mathbb{R}^{p \times p}$, calculated from x , is a *scatter matrix* if it is positive definite and affine equivariant, in the sense that

$$S(Ax + b) = AS(x)A'$$

for all full rank matrices $A \in \mathbb{R}^{p \times p}$ and vectors $b \in \mathbb{R}^p$.

Scatter matrices are a generalization of the regular covariance matrix $\Sigma := \text{Cov}(x)$, which clearly satisfies the desired equation. Some scatter matrices, for example the covariance matrix, have an additional independence property.

Definition 3. A scatter matrix S is said to have the *independence property* if $S(x)$ is diagonal for all random vectors x with independent components.

Now, a question rises, how can we find scatter matrices with the independence property? Besides the covariance matrix, another well-known example is the FOBI-matrix (used in an ICA method named fourth order blind identification [5]) $S_{\text{FOBI}} = \mathbb{E}[\tilde{x}\tilde{x}'\Sigma^{-1}\tilde{x}\tilde{x}']$, where $\tilde{x} := x - \mathbb{E}(x)$ and Σ denotes the covariance matrix of x . Moreover, further scatter matrices with the independence property can be obtained via the process call symmetrization, and we next state [37, Theorem 1] defining *symmetrized scatter matrices*

Theorem 1. [37] Let S be a scatter matrix and x_1, x_2 two independent copies of a random vector x . Then the matrix

$$S_s(x) := S(x_1 - x_2)$$

has the independence property.

On the sample level, the symmetrized scatter matrix can be calculated by applying S to the sample of all n^2 pairwise differences $x_i - x_j$ (where $i, j = 1, 2, \dots, n$) of the original observations.

Next, we define the independent component (IC) model using a general location vector and scatter matrix.

Definition 4. Let T be a location vector and let S_1 and S_2 be two scatter matrices with the independence property. A random vector $x \in \mathbb{R}^p$ is said to have IC-model with respect to T, S_1, S_2 if

$$x = \Omega z + \mu,$$

where the random vector $z \in \mathbb{R}^p$ has independent components, $T(z) = 0$, $S_1(z) = I_p$ and $S_2(z)$ is a diagonal matrix with elements $d_1 > \dots > d_p > 0$.

One could relax the assumptions to allow non-strict inequalities for the d_j , but this would lead to non-identifiable components, and we assume their strictness throughout this work. Now [37, Theorem 2] gives us a way to perform ICA, i.e., to estimate the source vector z , in such a case using matrix decompositions. This procedure is equivalent to ICS [43] with the choice S_1, S_2 of scatter matrices.

Theorem 2. [37] *Let x have an IC-model with respect to T, S_1 and S_2 . Let us define*

$$B(x) = S_1(x)^{-1/2} \left[U_2 \left(S_1(x)^{-1/2} x \right) \right],$$

where $U_2(x)$ is the matrix of eigenvectors of $S_2(x)$ (in the order of decreasing eigenvalues). Then

$$B(x)'(x - T(x)) = Jz$$

for some a diagonal matrix J with elements ± 1 .

In Theorem 2 the location vector T is used simply to fix the location of the independent components. Even without T , the ICs could be estimated up to location as $B(x)'x$ and, as such, we focus solely on the scatter matrices S_1, S_2 in the following, disregarding the location estimation. Independent component analysis based on Theorem 2, using symmetrized scatter matrices as the scatter matrices, is discussed in [42]. Finally, we note that Theorem 2 indeed states that any two scatter matrices with the independence property can be used to solve the IC problem on the population level. However, these scatter matrices might involve various assumptions and their finite-sample properties can still be different. Later we focus on a particular class of scatters that allows us to solve the problem in an outlier-resistant way.

2.2. Regression formulation for scatter matrix ICA

Fix next two scatter matrices, S_1, S_2 , both having the independence property. Computing the respective IC solution is simple to do via eigendecompositions as specified in Theorem 2, but we next present still an alternative way of obtaining the same solution, originally presented in the context of sufficient dimension reduction in [29]. The reason for introducing this auxiliary (and more complex) way of obtaining the solution has the benefit that it can be combined with sparsity in a natural way.

For $k \in 1, \dots, p$, let $U_k \in \mathbb{R}^{p \times k}$ denote the matrix comprising of the first k columns of $U_2 \left(S_1(x)^{-1/2} x \right)$.

Theorem 3. *Let $r_j \in \mathbb{R}^p$ denote the columns of $S_2(x)^{1/2}$. Then, the minimizers of*

$$\sum_{j=1}^p \|S_1(x)^{-1/2} r_j - AB' r_j\|_2^2$$

over $A, B \in \mathbb{R}^{p \times k}$, $A'A = I_k$, are precisely the pairs

$$(A, B) = (U_k O_k, S_1(x)^{-1/2} U_k O_k),$$

where O_k is any $k \times k$ orthogonal matrix.

Proof of Theorem 3. Simplifying the objective function, we see that the problem is equivalent to minimizing

$$-2\text{tr}(B'S_2(x)S_1^{-1/2}(x)A) + \text{tr}(B'S_2(x)B).$$

Differentiating this with respect to B , we get the gradient

$$-2S_2(x)S_1^{-1/2}A + 2S_2B.$$

The positive definiteness of S_2 thus shows that the minimizing value of B satisfies $B = S_1^{-1/2}(x)A$. Plugging this back in to the objective function, we see that the optimal A maximizes the map

$$A \mapsto \text{tr}(A'S_1^{-1/2}(x)S_2(x)S_1^{-1/2}(x)A),$$

over $A \in \mathbb{R}^{p \times k}$, $A'A = I_k$. By [21, Corollary 4.3.39], all maximizers are thus of the form $A = V_k O_k$ where $V_k \in \mathbb{R}^{p \times k}$ contain first k eigenvectors of $S_1^{-1/2}(x)S_2(x)S_1^{-1/2}(x)$ as its columns and O_k is an arbitrary $k \times k$ orthogonal matrix. By the affine equivariance of scatter matrices, $U_2 \left(S_1(x)^{-1/2} x \right)$ in Theorem 2 contains the p eigenvectors of $S_2(S_1^{-1/2}(x)x) = S_1^{-1/2}(x)S_2(x)S_1^{-1/2}(x)$, showing that $V_k = U_k$ (up to sign), and concluding the proof. \square

Two notes are in order: (i) Theorem 3 essentially converts the IC problem into minimization of a specific sum of squares. In the next section, we show how this minimization can be carried out using alternative least squares, allowing the sparsification of the solution through an ℓ_1 -penalty. (ii) All minimizers B of the objective function in Theorem 3 satisfy $\text{col}(B) = \text{col}(B(x))$ where $\text{col}(\cdot)$ denotes the column space and $B(x)$ is as in Theorem 2. As such, the solution in Theorem 3 is slightly less general than the original IC solution in Theorem 2 in that the former captures only the space spanned by the first k independent components, not their individual directions. Interestingly, this ambiguity is unavoidable and occurs even though our ICs have differing “kurtoses” d_1, \dots, d_p in Definition 4. Naturally, this ambiguity vanishes when $k = 1$ (the only 1×1 orthogonal matrices are the scalars ± 1), and to avoid it also in the case $k > 1$, we later in Section 3 propose a correction (lines 12–13 in Algorithm 1) that corrects for the presence of the orthogonal transformation O_k in our algorithm.

Finally, we remark that this O_k -ambiguity applies also to Theorem 3 in [50] and Propositions 1 and 2 in [29] but, likely due to an oversight, the authors have missed it. However, this omission was noted later in Remark II.1 in [10].

2.3. Symmetrized robust scatter matrices

Having observed how the ICA solution can be found using two scatter matrices, let us now take a look at one class of robust scatter matrices, robust M -estimators. By robust we mean that small deviations from assumptions do not impair the model’s performance too much and large deviations from model do not cause a catastrophe [23]. For us, the interesting deviation from assumptions is the existence of outliers. Since we will eventually focus exclusively on symmetrized scatter matrices, we assume, without loss of generality, that the true location of the data x_1, \dots, x_n is zero.

Now, given a function $\rho : \mathbb{R} \rightarrow \mathbb{R}$, the corresponding M -estimator scatter matrix S is found by minimizing

$$L(S) = \frac{1}{n} \sum_{i=1}^n \{\rho(x_i' S^{-1} x_i) - \rho(x_i' x_i)\} + \ln \det S.$$

This expression originally comes from the maximum likelihood estimation of an elliptic distribution with density proportional to $\det(S^{-1}) \exp(-\rho(x' S^{-1} x))$. The function ρ is typically assumed to satisfy various regularity conditions, see [13, 15]. One common choice for the function ρ is $\rho_{\nu,p}(z) = (\nu + p) \ln(\nu + z)$ which comes from the p -variate t -distribution with $\nu > 0$ degrees of freedom.

The above minimization problem leads to an estimating equation

$$\frac{1}{n} \sum_{i=1}^n w(\|S^{-1/2} x_i\|^2) \|S^{-1/2} x_i\|^{-2} S^{-1/2} x_i x_i' S^{-1/2} = I_p, \quad (1)$$

where $w(z) = \rho'(z)z$ is called a weight function. M -estimators are often defined in terms of the function w instead of the function ρ . Common choices for w are [41] $w(z) = z$ giving the regular covariance matrix and $w(z) = p$ giving Tyler’s M -estimator [43]. Another common choice is the Huber’s M -estimator

$$w(z) = \begin{cases} |z|/\sigma, & \text{for } |z| \leq c \\ c/\sigma, & \text{for } |z| > c, \end{cases}$$

where the tuning constant c is chosen to control $\mathbb{P}(\chi_p^2 \leq c^2/2)$ and the scaling factor σ is chosen so that $\mathbb{E}[w(\|x\|^2)] = p$ for $x \sim N(0, I_p)$.

Now we can define symmetrized M -estimates by replacing observations x_i by pairwise differences $x_i - x_j$ (similarly, the averaging $\frac{1}{n} \sum_{i=1}^n$ in (1) is replaced by the double sum $\frac{2}{n(n-1)} \sum_{i < j}$). In this work we use symmetrized versions of two of the robust scatter matrix families discussed above, the MLE of t -distribution [13] and Huber’s M -estimator [41]. These have been implemented in the R-packages `fastM` [14] and `ICSNP` [36], respectively.

2.4. Measuring robustness

The two most common ways to measure robustness of a statistic are the breakdown point and influence function. Breakdown point describes how big proportion of observations can be outliers without the statistic having arbitrary

large/small values. Let T be a statistic taking values in some normed space, X a sample and X_ε a sample with proportion ε of the observation replaced with arbitrary values. Let

$$b(X_\varepsilon, T) = \sup_{X_\varepsilon} \|T(X) - T(X_\varepsilon)\|$$

be the maximal bias. Now we can define the finite-sample breakdown point of T as in [11], as

$$\varepsilon^* = \inf\{\varepsilon \mid b(X_\varepsilon, T) = \infty\}.$$

As an example of the breakdown point in the case of simple estimators, consider the sample mean and sample median. Sample mean has the lowest possible breakdown point because replacing just one observation with arbitrarily high values can increase the mean without any limit. On the other hand, to increase the sample median to arbitrarily high value requires replacing half of the sample, making its breakdown point $1/2$.

It is well known that, in general, M -estimators have no greater breakdown points than $1/(p+1)$ [31]. Still [44] shows that when the contaminating points are assumed to not lay in any low dimensional hyperplane (called coplanar contamination), the M -estimate can have a breakdown point close to $1/2$. In general symmetrization can be expected to lower the breakdown point of a scatter matrix, see [16], but, as our simulations later in Section 4 show that robust scatters, even when symmetrized, tolerate outliers particularly well.

Another measure of robustness is the influence function for a statistic T . Let Q be a probability distribution and $Q_\varepsilon = (1-\varepsilon)Q + \varepsilon\Delta_x$ be an ε -contaminated version of Q , where Δ_x is a distribution with all probability mass concentrated to the point x . Then the influence function of T for a point x can be defined as

$$IF(x; T, Q) = \lim_{\varepsilon \rightarrow 0} \frac{T(Q_\varepsilon) - T(Q)}{\varepsilon}.$$

The influence function measures how much a (infinitely) small change in the distribution at a point x can change the value of the statistic T . One way to characterize a robust statistic is to require that it has a bounded influence function which means that no single contamination at any point can influence the statistic by an unlimited amount.

It follows from Theorem 3 in [41] that symmetrized M -estimators have bounded influence function when the weight function w is bounded. This is the case for symmetrized Huber's M -estimator and the MLE of t -distribution with $w(z) = \rho'(z)z = (\nu+p)(1+\frac{z^2}{\nu})^{-1}$.

3. Sparse and robust ICA

3.1. Algorithm

Based on the concepts in the previous section, we next propose an algorithm for obtaining a robust and sparse ICA solution. Let S_1 and S_2 be two robust scatter matrices with the independence property, $r_j \in \mathbb{R}^p$ denote the columns of $S_2(x)^{1/2}$ and $\lambda_m \geq 0$ be the sparsity penalization parameter corresponding to the m th independent component. Then, the matrix $B = (\beta_1, \dots, \beta_k)$ part of the minimizer $A, B \in \mathbb{R}^{p \times k}$ ($A'A = I_k$) of

$$\sum_{j=1}^p \|S_1(x)^{-1/2} r_j - AB' r_j\|_2^2 + \sum_{m=1}^k \lambda_m \|\beta_m\|_1 \quad (2)$$

is the sparse invariant coordinate selection estimate, up to multiplying from right by some $k \times k$ orthogonal matrix O_k (see Theorem 3). In practice, one usually directly chooses the desired numbers of non-zero components r (usually taken to be the same for all components) and the penalization parameters λ_j are then determined implicitly based on r .

A procedure for minimizing (2) is shown in Algorithm 1. The command `fix_signs` (lines 3, 9) flips the signs of the columns β_j of B so that the first non-zero element in each column is positive. This is done to eliminate the effect of signs changing between iterations of the repeat-until-loop. Line number 7 comes from being able to represent (2) (for a fixed A) as

$$\text{tr}((I_p - AA')S_1^{-1}S_2) + \|S_2^{1/2}S_1^{-1/2}A - S_2^{1/2}B\|^2 + \sum_{m=1}^k \lambda_m \|\beta_m\|_1,$$

Algorithm 1: Sparse invariant coordinate selection

Data: Scatter matrices $S_1, S_2 \in \mathbb{R}^{p \times p}$
Parameters: Number of invariant coordinates k
The numbers of non-zero coordinates (r_1, \dots, r_k)
Result: Matrix of the coefficient vectors $B = (\beta_1, \dots, \beta_k) \in \mathbb{R}^{p \times k}$

- 1 Let $A = (\alpha_1, \dots, \alpha_k) \in \mathbb{R}^{p \times k}$ be the usual non-penalized ICS estimate with respect to S_1 and S_2 ;
- 2 $B = S_1^{-\frac{1}{2}} A$;
- 3 $B = \text{fix_signs}(B)$;
- 4 **repeat**
- 5 $B_{temp} = B$;
- 6 **for** $j \in \{1, 2, \dots, k\}$ **do**
- 7 $\beta_j = \arg \min_{\beta_j} \left\{ \sum \|S_2^{\frac{1}{2}} S_1^{-\frac{1}{2}} \alpha_j - S_2^{\frac{1}{2}} \beta_j\|_2^2 + \lambda_j \|\beta_j\|_1 \right\}$;
- 8 **end**
- 9 $B = \text{fix_signs}(B)$;
- 10 Calculate the singular value decomposition $S_1^{-\frac{1}{2}} S_2 B = U D V'$;
- 11 $A_0 = U V'$;
- 12 Calculate the eigendecomposition $A_0' S_1^{-\frac{1}{2}} S_2 S_1^{-\frac{1}{2}} A_0 = O_k \Delta O_k'$;
- 13 $A = A_0 O_k$;
- 14 **until** $\|B - B_{temp}\|_{2,2} < 10^{-6}$;
- 15 **return** B ;

and we use the function `solvbeta` from the R-package `elasticnet` [49] to solve this LASSO-type problem (this function allows us to choose the number of non-zero components r instead of the penalization parameters λ_j).

The estimate for A calculated on lines 10–11 comes from representing (2) (for fixed B , so without needing the penalty term) as

$$\sum_{j=1}^p \|S_1(x)^{-1/2} r_j - A B' r_j\|_2^2 = \|S_1(x)^{-1/2} S_2^{1/2} - A B' S_2^{1/2}\|_2^2 = \|S_2^{1/2} S_1(x)^{-1/2} - S_2^{1/2} S_1(x)^{-1/2} S_1(x)^{1/2} B A'\|_2^2$$

and using the reduced rank Procrustes rotation [50, Theorem 4] to minimize this expression with respect to A . As this estimate is only calculated up to the rotation O_k , we choose O_k (lines 12–13) so that A diagonalizes $S_1^{-\frac{1}{2}} S_2 S_1^{-\frac{1}{2}}$. This choice thus corresponds to how the solution to the joint diagonalization behaves in the regular ICS.

Algorithm 1 thus produces a sparse matrix B (whose sparsity level is controlled by the parameters r_1, \dots, r_k), using which the independent components are obtained as $B' x_i$.

3.2. Consistency of SICS

We next establish conditions under which the proposed sparse and robust ICA yields consistent estimates of the independent components. The result is stated in terms of two arbitrary scatter matrices S_1, S_2 , implying that it actually applies not just in ICA, but in the wider framework of ICS, including also the sufficient dimension reduction methodology of [29]. For simplicity, we restrict in the result to the case $k = 1$, meaning that we are estimating the first IC (or invariant coordinate, in the general case) only. Given sample estimates S_{n1}, S_{n2} of the two scatter matrices, we let $b_{n,\lambda_n} \in \mathbb{R}^p$ denote the minimizing value of β_1 (the first column of B) in the sample version of the optimization problem (2) when the penalization parameter is $\lambda_1 \equiv \lambda_n$. Similarly, we let $b \in \mathbb{R}^p$ denote the minimizing value of β_1 in the corresponding population level problem with no penalization. By Theorems 2 and 3, when S_1, S_2 have the independence property, the vector b thus equals the first row of the unmixing matrix Ω^{-1} , up to sign. As is typical in convergence results related to LASSO-like methods [7, 17], a necessary condition for the convergence of b_{n,λ_n} to b is that the penalty parameter λ_{n1} vanishes at an appropriate rate as $n \rightarrow \infty$. Theorem 4 below is proven in several steps in Appendix A and follows from Theorem 5 therein, by selecting $a_n := 1/c_n$.

Theorem 4. Let S_{n_1}, S_{n_2} be two $p \times p$ sample scatter matrices satisfying

$$c_n(S_{n_1} - S_1) = \mathcal{O}_p(1) \quad \text{and} \quad c_n(S_{n_2} - S_2) = \mathcal{O}_p(1)$$

for some sequence c_n satisfying $c_n \rightarrow \infty$ and some positive definite S_1, S_2 . Let $\lambda_{n_1} \rightarrow 0$ be such that $\lambda_{n_1} c_n \rightarrow 0$. Then,

$$c_n \|s_n b_{n, \lambda_n} - b\|_2 = \mathcal{O}_p(1),$$

for some sequence $s_n \in \{-1, 1\}$ of signs.

In a typical case, the convergence rate of the scatter estimates would be $c_n = \sqrt{n}$, see e.g. [27, 32], meaning that the ‘‘optimal’’ (most sparsity inducing) choice of the penalization parameter is $\lambda_{n_1} = n^{-1/2-\varepsilon}$ for some arbitrarily small $\varepsilon > 0$. By Theorem 4, this choice then leads to b_{n, λ_n} also inheriting the convergence rate \sqrt{n} from the two scatter matrices.

We still give a short summary of the techniques of proof used in showing Theorem 4: We break the problem down in the tasks of separately controlling the errors between b_{n, λ_n} and $b_{n, 0}$ and between $b_{n, 0}$ and b . The latter task does not depend on the sparsity parameter and is based on manipulating the matrix form of the generalized eigendecomposition of S_{n_2} w.r.t. S_{n_1} to establish the convergence in a specific coordinate system and then extending the result to the general case via affine equivariance (Lemma 4). The former task (error between b_{n, λ_n} and $b_{n, 0}$) is more tedious, and involves obtaining a sequence of lower bounds for the difference of the two objective functions and showing that, as soon as λ_{n_1} vanishes at a suitable rate, the corresponding minimizers are within an ε -neighbourhood of each other with increasing probability. The combining of the two results then yields Theorem 4.

4. Simulations

4.1. Simulation study #1

We investigated the performance of the proposed method SICS with simulations. The task was to estimate the sparse unmixing matrix Ω^{-1} for a data matrix $X = (x_1, \dots, x_n)'$ generated from the IC model $X = Z\Omega'$ where $Z = (z_1, \dots, z_n)'$. In every iteration, we first generated a random unmixing matrix $\Omega^{-1} \in \mathbb{R}^{p \times p}$, where every row has a preset number q of non-zero elements coming from the Uniform($[-3, -1] \cup [1, 3]$)-distribution. Then, we generated a random source matrix $Z \in \mathbb{R}^{n \times p}$ with the elements of the first column coming from the standardized Laplace distribution, the second column coming from standardized uniform distribution and rest coming from the standard normal distribution. Last, we generated the data matrix $X = Z\Omega'$ using Z and Ω . We contaminated the data matrix X by replacing 5% of the rows with observations coming from $N(0, 3)$. All simulations were also run similarly to the non-contaminated datasets to evaluate the effect of the contamination to the estimators. We used different variations of proposed SICS algorithm to estimate the coefficient vector β_1 of the first independent component and calculated its absolute distance to the true first row of the matrix Ω . Because the sign of the coefficient vector is arbitrary, distance to vector with flipped signs was used if it was smaller. Then we took the median of this over N iterations.

The methods to compare were SICS with four different numbers of estimated non-zero coefficients r : full p (non-sparse estimate), true q (oracle estimate), $q + 3$ and ‘‘forced $q + 3$ ’’ where all p coefficients were first estimated in a non-sparse way and then the $p - q - 3$ with the smallest absolute values were set to zero (making it a thresholding estimate). All of those were run with a non-robust pair of scatter matrices, the covariance matrix and the FOBI matrix, and a robust pair, symmetrized t -distribution based ($\nu = 1$) and symmetrized Huber’s M -estimator (where c is chosen so that $\mathbb{P}(\chi_p^2 \leq c^2/2) = 0.9$).

First, we chose the number of variables to be $p = 15$, of which non-zero $q = 7$. We varied the number of observations $n = 500, 1000, 1500, 2000, 2500$ and took $N = 1000$ repetitions for each n . The results are presented in Figure 1. When the dataset is contaminated, methods based on robust scatter matrices perform clearly better than non-robust, as one could expect. SICS with $r = q + 3$ performs the best after $n = 1500$. With non-contaminated data, the difference between robust and non-robust is not as clear as with contaminated data, but, overall, robust variants still seem to perform a better than the non-robust. With high n , we see that all robust methods except the choice $r = q$ perform about the same. Overall we can conclude that higher sample size n increases performance, as expected, and that the robust variants outmatch the non-robust ones.

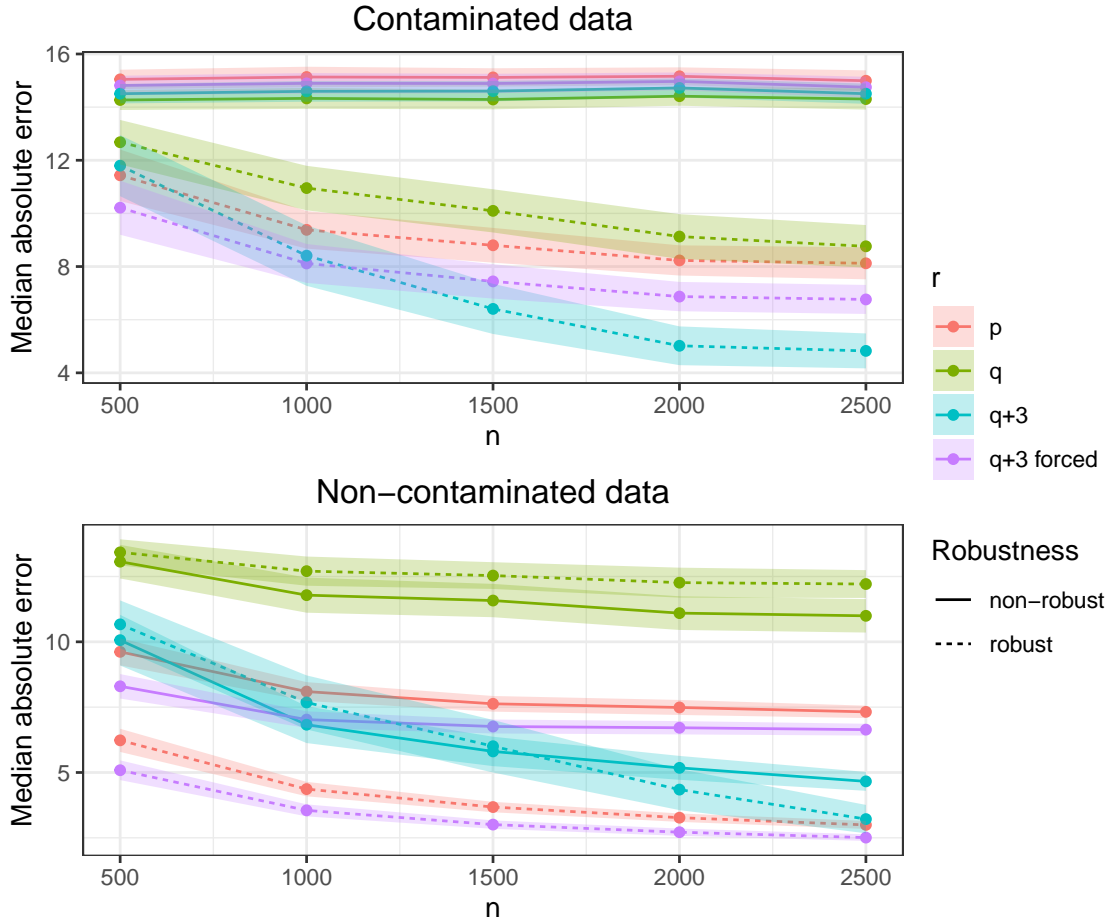


Fig. 1: Median absolute error by sample size for different methods. The error ribbon has width $0.2 \times \text{MAD}$

Then, we chose the number of variables to be $p = 15$ and the number of observations to be $n = 1500$. We varied the number of non-zero coefficients $q = 2, 3, 5, 8, 11, 15$ for again $N = 1000$ repetitions for each q . The results are presented in Figure 2, where the y-axis is standardized by dividing by q which is proportional to the l_1 -norm of a constant vector with q non-zero coefficients. We can again see that with contaminated data robust variants work best. When the number of non-zero coefficients is small, sparse variants work better, as one could guess. We can also see again that these differences, and similarly the effect of the robustness, are not so clear in the case of the non-contaminated data.

4.2. Simulation study #2

The purpose of our second simulation is to investigate the optimal choice of r (sparsity level of the estimate) for a given q (the true sparsity level). Naturally, it is clear that $r \geq q$ is the minimal requirement for successful estimation but, based on the previous simulations, having $r > q$ is actually preferable and we next study what amount of “overestimation” is optimal for finite samples. We generated data from the same model as earlier, with $n = 1000$, a contamination level equal to 5%, dimensions $p = 10, 15, 20$ and $q = \lfloor \alpha p \rfloor$ for $\alpha = 0.1, \dots, 1.0$. We then estimated the first IC using the same robust pair of scatter matrices as in the earlier simulation, separately for each $r = 1, \dots, p$, and recorded the value of r , denoted as r_{opt} yielding the smallest median absolute error. The simulation was repeated 200 times for each combination of p, α , and in Figure 3 we give the average values of r_{opt}/p over the replicates.

The results reveal that the optimal choice of r (as a proportion of p) depends very little on the dimension p . Moreover, the amount of optimal overestimation depends on the true sparsity in the following manner: if there are

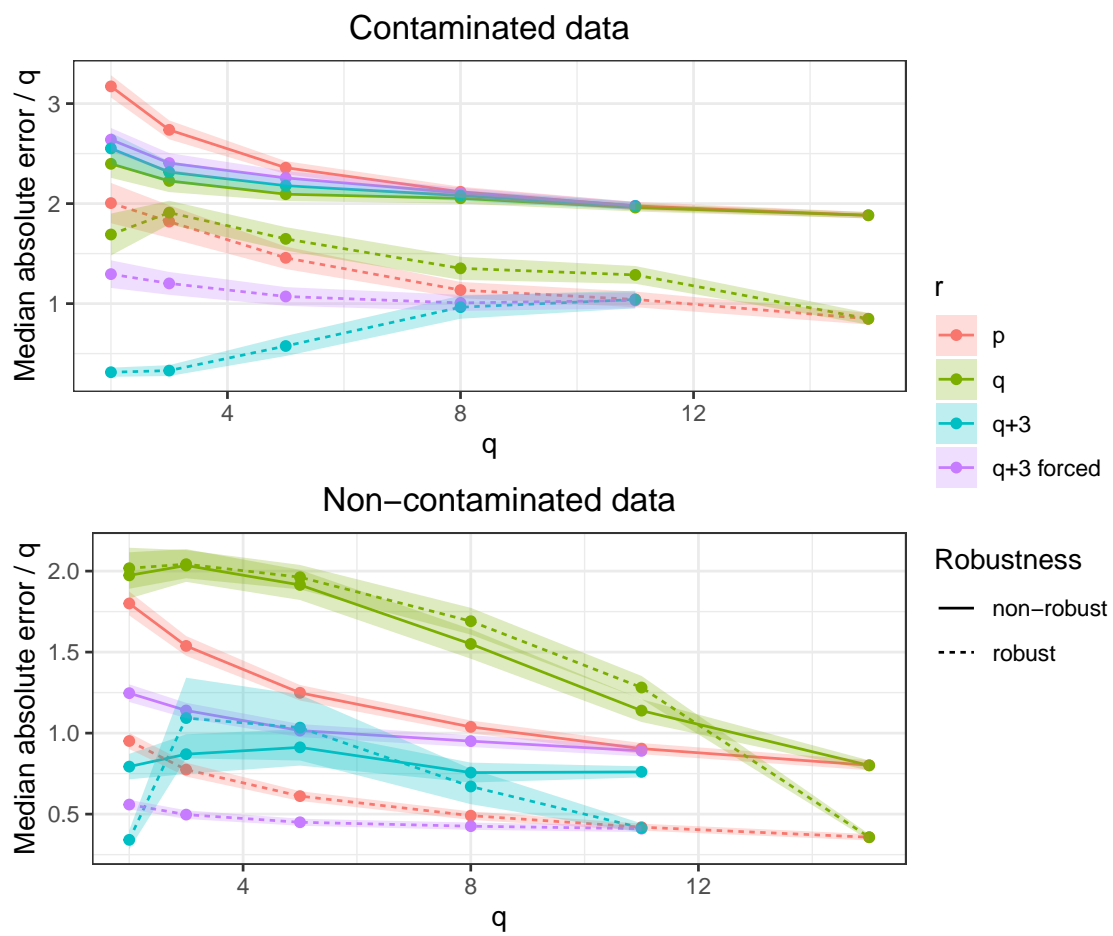


Fig. 2: Median absolute error by number of non-zero coefficients for different methods. The error ribbon has width $0.2 \times \text{MAD}$. Error is scaled by dividing by q .

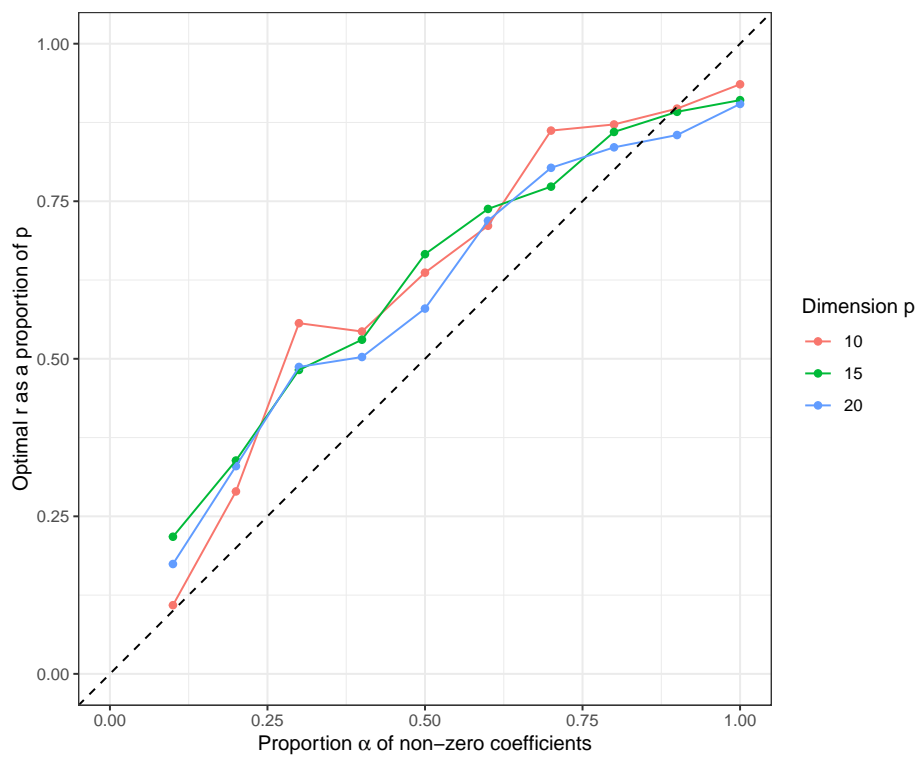


Fig. 3: The plot shows the average optimal values of r (as proportions of p) as a function of α , the true proportion of non-zero coefficients in the first IC. The different lines correspond to different dimensions p .

only a few true non-zero coefficients, then greater overestimation is preferable, and vice versa. See Section 6 for discussion on the choice of r in practice.

5. Robust causal discovery

We next demonstrate how the proposed method can be used in robust construction of causal graphs. Given a dataset with p variables, the objective in *causal discovery* is to form a directed acyclic graph whose nodes are the variables and whose edges represent causal relations between the variables [39]. The acyclicity and directedness of the graph then ensures that “effects cannot precede causes”. [40] showed the remarkable fact that ICA can be used for non-Gaussian linear causal discovery. Essentially, this is because a linear non-Gaussian causal model between the elements of a random p -vector x can be written as $x = Bx + \varepsilon$, where ε represents measurement noise with non-Gaussian independent components and the $p \times p$ matrix B is strictly lower triangular. By rearranging the terms, we observe that this is actually an IC model, $x = (I - B)^{-1}\varepsilon$ and thus estimable with ICA.

In general, the unmixing matrix estimates produced by ICA-methods are not lower triangular (or permutations thereof) and, as such, typical ICA solutions do not correspond to causal graphs. However, this can be forced with the following two steps: (i) By using a sparse ICA method, the estimate of $I - B$ becomes sparser and usually closer to being a permutation of a lower triangular matrix, see [20]. (ii) By permuting the result of a sparse ICA method to be as lower triangular as possible and afterwards pruning the excess elements to zero, e.g., with the efficient and scalable algorithm in [22]. See also [33] for a second-order ICA method whose identifiability constraints make it naturally suited to causal discovery.

In this experiment we apply the previous causal discovery approach to the `diabetes` dataset available in the R-package `elasticnet` [49]. The data consist of the measurements of 10 baseline covariates (such as age, sex and bmi) and a response variable (disease progression score), for $n = 442$ patients. To discover causal relationships between this set of $p = 11$ variables, we use our proposed method to construct causal graphs as described above, see [22] for details of the permutation and pruning algorithm. We distinguish two versions of our method: for the first S_1, S_2 equal the covariance matrix and the matrix of fourth moments (non-robust method) and for the second S_1, S_2 equal the symmetrized MLE of t_1 -distribution and the symmetrized Huber’s M -estimator with the tuning parameter value 0.9 (robust method). In both cases, we estimate a full set of p independent components with $r = 7$ non-zero coefficients per component. As each produced causal graph can be seen as a single “point estimate”, we bootstrap the original data set 1000 times, and use both methods (non-robust and robust) to estimate the causal graph for each bootstrap replicate. The final, aggregated graphs are then formed by retaining only those directed edges which are present in at least 40% of the bootstrap graphs, separately for both methods. This low percentage was chosen since the produced graphs exhibited quite a lot of variability, which stems from the fact that the sample size $n = 442$ is relatively small from the viewpoint of ICA.

The obtained causal graphs are shown in Figure 4 and show that both methods more or less agree on the causal structure of the data, indirectly indicating that the data is not likely to contain significant outliers (which likely stems from the fact that the data represents a curated clinical study). The main feature of interest is that most of the 10 explanatory variables are estimated to be causes of the disease progression. Additionally, a relation between the covariates LDL and TC was discovered. We note that these plots should not be interpreted as the full causal graphs between the 11 variables, but rather as estimates of the set of *strongest causal relationships* between the variables.

We next take these findings as the ground truth, and continue the experiment by creating a contaminated version of the data set, obtained by randomly selecting 10% of the subjects and replacing all their measurements with i.i.d. Gaussian noise with standard deviation $\sigma = 20$. We then applied the same causal discovery approach to this contaminated data set, with the hopes of still being able to find the relevant structure, despite the contamination. The bootstrapped causal graphs estimated from the contaminated data are shown in Figure 5 and reveal that the structure of the non-robust graph has completely changed, with only two of the original edges remaining. That is, the outliers have made it impossible for standard, non-robust ICA to find almost any causal relations. Whereas, the graph from robust and sparse ICA retains most of the connections, in particular the edges between the disease progression and the covariates AGE, SEX, BMI, MAP, TC, LDL and GLU. We thus conclude that sparse and robust ICA offers a reliable and outlier-resistant method for linear causal discovery.

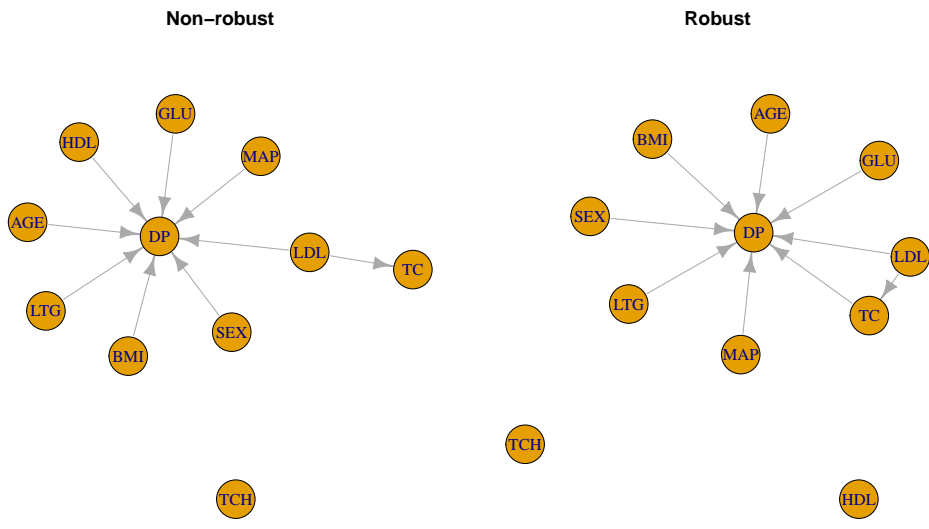


Fig. 4: The aggregated causal graphs estimated from the diabetes data by the non-robust and robust method. The variable abbreviations are: DP = disease progression index, AGE = age, SEX = sex, BMI = body mass index, MAP = mean arterial blood pressure, whereas TC, LDL, HDL, TCH, LTG, GLU correspond to specific blood serum measurements.

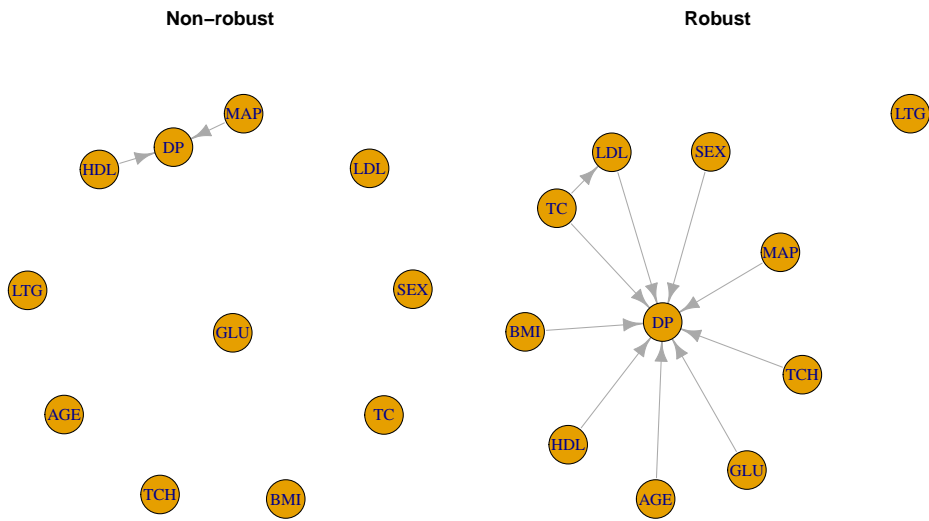


Fig. 5: The aggregated causal graphs estimated from the artificially contaminated diabetes data by the non-robust and robust method. See the caption of Figure 4 for the variable abbreviations.

6. Discussion

We conclude with a discussion about some practical matters and topics for future study. An important choice one has to make when using SICS is selecting the number of non-zero coefficients r (usually chosen to be the same for all estimated components). Based on simulations, choosing the actual underlying value q is not optimal, but the best option is to choose a value around 10 – 20% greater than q . This is because then there is some room for error before a coefficient, which is actually non-zero, is estimated to be zero. It follows that using $r < q$ (for example $r = q - 1$) results in clearly bad performance (this was tested in the simulation but not shown). Choosing r based on the real value q is not usually possible and can be done only in applications where one has some a priori information of the real value q .

Often in practice, this choice is made not by trying to guess the underlying value q , but by choosing the amount of sparsity the user wants. Reasons for sparsity are easier interpretability, as there are less coefficients to interpret, and trying to avoid overfitting. It can also be beneficial to try different values of r . The most typical way of choosing the number of non-zero coefficients (or the amount of regularization), cross-validation, is not possible in our unsupervised setting.

Computationally, the most demanding part is the calculation of robust scatter matrices. This is because the symmetrized scatter matrices are calculated with pairwise differences and there are n^2 of those instead of the amount n of original data points. One possible solution to this could be to use only a subset of the pairwise distances [12]. We did not try this in the current context because the dataset sizes were manageable without.

The consistency result, Theorem 4, is formulated only for estimating one component ($k = 1$). This case is simpler than the general case because one does not have to estimate the rotation matrix O_k . We still expect the result to hold for larger k since the matrix O_k consists of eigenvectors of a product of the scatter matrices and the estimated coefficients, which are all either assumed or proven to converge at the rate c_n , which is thus expected to be inherited by the estimate of O_k as well.

Acknowledgments

The work of LH and JV was supported by the Research Council of Finland (grants 347501, 353769). The authors would like to thank Andreas Artemiou who brought the work by [29] to their attention.

Appendix A. Proof of Theorem 4

In this section we prove Theorem 4 in several steps. For clarity (to avoid the use of multiple subscripts), the notation in the proofs differs slightly from the main text.

We assume that M_n, G_n are symmetric $p \times p$ matrices such that

$$M_n \rightarrow_p M, \quad G_n \rightarrow_p G,$$

as $n \rightarrow \infty$, where M, G are symmetric and positive definite $p \times p$ matrices. The first, second and last eigenvalues of $G_n^{-1/2} M_n G_n^{-1/2}$ are denoted in the following by ρ_n, ψ_n, Ω_n , respectively. The population counterparts of these are denoted by ρ, ψ, Ω and we assume that $\rho > \psi$ and $\Omega > 0$. The population and sample eigenvectors corresponding to the leading eigenvalues ρ_n, ρ are denoted by $u_n, u \in \mathbb{R}^p$, respectively. Finally, we denote the smallest eigenvalues of G_n and G as α_n and $\alpha > 0$, respectively.

The following lemma and corollary follow from the results of [29] and we thus omit their proofs.

Lemma 1. For $a, b \in \mathbb{R}^p$, $\|a\|_2 = 1$, we have

$$\sum_{i=1}^p \|G^{-1/2} r_i - ab' r_i\|_2^2 = \text{tr}(G^{-1/2} M G^{-1/2}) - 2b' M G^{-1/2} a + b' M b,$$

where $(r_1, \dots, r_p) = M^{1/2}$.

Corollary 1. *The minimizer (α, β) of*

$$(a, b) \mapsto \sum_{i=1}^p \|G^{-1/2} r_i - ab' r_i\|_2^2,$$

over $a, b \in \mathbb{R}^p$, $\|a\|_2 = 1$ is

$$\alpha = u \quad \text{and} \quad \beta = G^{-1/2} u.$$

We next equip the objective function in Corollary 1 with an ℓ_1 -penalty for the parameter b . This leads to the following three versions of the optimization problem. The first one is a sample problem with the penalty parameter (sequence) λ_n , the second one is the non-penalized sample problem, and the third one is simply the population-level problem from Corollary 1.

- **Version I:**

$$(a_{n,\lambda_n}, b_{n,\lambda_n}) = \operatorname{argmin} f_{n,\lambda_n}(a, b), \quad a, b \in \mathbb{R}^p, \|a\|_2 = 1,$$

where $f_{n,\lambda_n}(a, b) = -2b' M_n G_n^{-1/2} a + b' M_n b + \lambda_n \|b\|_1$.

- **Version II:**

$$(a_{n,0}, b_{n,0}) = \operatorname{argmin} f_{n,0}(a, b), \quad a, b \in \mathbb{R}^p, \|a\|_2 = 1,$$

where $f_{n,0}$ is as in Version I above.

- **Version III:**

$$(\alpha, \beta) = \operatorname{argmin} f(a, b), \quad a, b \in \mathbb{R}^p, \|a\|_2 = 1,$$

where $f(a, b) = -2b' M G^{-1/2} a + b' M b$.

Our objective is to show that, under suitable assumptions, $(a_{n,\lambda_n}, b_{n,\lambda_n})$ converges in probability to (α, β) . I.e., that the ℓ_1 -penalized problem gives consistent solutions. We do this by first showing that the solutions of Versions I and II are close and then doing the same for Versions II and III.

For a vector $m \in \mathbb{R}^p$, we define $a_{n,\lambda_n,m}^*$ to be the minimizer of the objective function

$$a \mapsto f_{n,\lambda_n}(a, b_{n,0} + m),$$

over $a \in \mathbb{R}^p$, $\|a\|_2 = 1$. As the objective function is symmetric in the sense that $f_{n,\lambda_n}(a, b) = f_{n,\lambda_n}(-a, -b)$, it is sufficient to restrict our attention to vectors $m \in \mathbb{R}^p$ such that $b_{n,0}' G_n (b_{n,0} + m) \geq 0$ (corresponding to a certain half-space of \mathbb{R}^p).

The next lemma quantifies the ‘‘cost’’ of using the perturbed point $(a_{n,\lambda_n,m}^*, b_{n,0} + m)$ as a candidate solution for the Version I of the optimization problem instead of the point $(a_{n,\lambda_n,0}^*, b_{n,0})$.

Lemma 2. *For any $m \in \mathbb{R}^p$ such that $b_{n,0}' G_n (b_{n,0} + m) \geq 0$, we have*

$$\begin{aligned} & f_{n,\lambda_n}(a_{n,\lambda_n,m}^*, b_{n,0} + m) - f_{n,\lambda_n}(a_{n,\lambda_n,0}^*, b_{n,0}) \\ & \geq \min\{C_{1n}, C_{2n}\} \|A_n^{-1}\|_2^{-2} \|G_n^{-1/2}\|_2^{-2} \|m\|_2^2 - \lambda_n \sqrt{p} \|m\|_2, \end{aligned}$$

where

$$\begin{aligned} C_{1n} & := 0.4 \rho_n \{\rho_2(A_n)^{-1} - 1\}, \\ C_{2n} & := (\sqrt{0.6} - \sqrt{0.4})^2 \rho_n, \end{aligned}$$

and $A_n := G_n^{-1/2} M_n G_n^{-1/2} / \rho_n$.

Proof of Lemma 2. Application of the Cauchy-Schwarz inequality reveals that

$$a_{n,\lambda_n,m}^* = \frac{\rho_n u_n + M_{n,0} G_n^{1/2} m}{\|\rho_n u_n + M_{n,0} G_n^{1/2} m\|_2}.$$

Consequently, for $m \in \mathbb{R}^p$,

$$\begin{aligned} & f_{n,\lambda_n}(a_{n,\lambda_n,m}^*, b_{n,0} + m) - f_{n,\lambda_n}(a_{n,\lambda_n,0}^*, b_{n,0}) \\ &= -2\|\rho_n u_n + M_{n,0} G_n^{1/2} m\|_2 + 2\rho_n + 2b'_{n,0} M_n m + m' M_n m \\ & \quad + \lambda_n (\|b_{n,0} + m\|_1 - \|b_{n,0}\|_1), \end{aligned} \tag{A.1}$$

where $M_{n,0} := G_n^{-1/2} M_n G_n^{-1/2}$ and ρ_n denotes the largest eigenvalue of this matrix. Let now $A_n := M_{n,0}/\rho_n$ and express m as $m = G_n^{-1/2} A_n^{-1} v$ for some $v \in \mathbb{R}^p$. Our earlier assumption that $b'_{n,0} G_n (b_{n,0} + m) \geq 0$ then takes the form

$$\begin{aligned} 0 &\leq b'_{n,0} G_n (b_{n,0} + m) \\ &= u'_n (u_n + G_n^{1/2} m) \\ &= 1 + u'_n A_n^{-1} v \\ &= 1 + u'_n v, \end{aligned}$$

as u_n is an eigenvector of A_n corresponding to the eigenvalue 1.

Then, we can write the first part of the right-hand side of (A.1) as

$$\begin{aligned} & -2\|\rho_n u_n + M_{n,0} G_n^{1/2} m\|_2 + 2\rho_n + 2b'_{n,0} M_n m + m' M_n m \\ &= \rho_n \{-2\|u_n + A_n G_n^{1/2} m\|_2 + 2 + 2u'_n A_n G_n^{1/2} m + m' G_n^{1/2} A_n G_n^{1/2} m\} \\ &= \rho_n \{-2\|u_n + v\|_2 + 2 + 2u'_n v + v' A_n^{-1} v\}. \end{aligned}$$

Then, have the following identity

$$(\|u_n + v\|_2 - 1)^2 = 1 + 2u'_n v + v' v - 2\|u_n + v\|_2 + 1.$$

Hence, we can write

$$\begin{aligned} & -2\|\rho_n u_n + M_{n,0} G_n^{1/2} m\|_2 + 2\rho_n + 2b'_{n,0} M_n m + m' M_n m \\ &= \rho_n \{(\|u_n + v\|_2 - 1)^2 + v' (A_n^{-1} - I_p) v\}. \end{aligned} \tag{A.2}$$

Now, as A_n has its eigenvalues in $[0, 1]$, then $A_n^{-1} - I_p$ has eigenvalues in $[0, \infty)$ with the eigenvector u_n corresponding to the eigenvalue 0. Decompose then v such that $v = P_n v + Q_n v$ where $P_n := u_n u'_n$ is the projection onto u_n and $Q_n := I_p - P_n$. As such, $P_n (A_n^{-1} - I_p) = 0$ and we have

$$\begin{aligned} v' (A_n^{-1} - I_p) v &= v' Q_n (A_n^{-1} - I_p) Q_n v \\ &= \|Q_n v\|_2^2 \frac{(Q_n v)'}{\|Q_n v\|_2} (A_n^{-1} - I_p) \frac{Q_n v}{\|Q_n v\|_2} \\ &\geq \|Q_n v\|_2^2 \rho_{p-1} (A_n^{-1} - I_p) \\ &= \|Q_n v\|_2^2 \{\rho_2(A_n)^{-1} - 1\}, \end{aligned}$$

where $\rho_k(B)$ denotes the k th largest eigenvalue of the matrix B .

We next derive a lower bound for the right-hand side of (A.2) (call it T_n in the following), dividing the treatment into two cases. Fixing an arbitrary $\varepsilon \in (0, 1/2)$, if $\|Q_n v\|^2 / \|v\|^2 \geq 0.5 - \varepsilon$, then the preceding paragraph shows that

$$\begin{aligned} T_n &\geq \rho_n \|Q_n v\|_2^2 \{\rho_2(A_n)^{-1} - 1\} \\ &\geq \rho_n \|v\|_2^2 (0.5 - \varepsilon) \{\rho_2(A_n)^{-1} - 1\}. \end{aligned}$$

Take next the complementary case $\|P_n v\|^2/\|v\|^2 > 0.5 + \varepsilon$. We consider two sub-cases (I) and (II). In the first one, we assume that $\|u_n + v\| \leq 1$. In this case we have

$$|1 - \|u_n + v\|| > 1 - \left\{1 + \|v\|^2 - \sqrt{2(1 + 2\varepsilon)}\|v\|\right\}^{1/2}. \quad (\text{A.3})$$

To see that this holds, we first observe that the quantity inside the square root can be written as

$$(1 - \|v\|)^2 + \|v\|\{2 - \sqrt{2(1 + 2\varepsilon)}\},$$

where $2(1 + 2\varepsilon) < 4$, making (A.3) well-defined. Now, some simplification shows that (A.3) is equivalent to

$$1 + 2u'_n v + \|v\|^2 < 1 + \|v\|^2 - \sqrt{2(1 + 2\varepsilon)}\|v\|,$$

which in turn is equivalent to $u'_n v < -\|v\|(0.5 + \varepsilon)^{1/2}$, which we next show to hold. Because $\|P_n v\|^2 = (u'_n v)^2$, our assumption writes as $(u'_n v)^2 > \|v\|^2(0.5 + \varepsilon)$. As $\|u_n + v\| \leq 1$ implies that $u'_n v \leq 0$, the case $u'_n v > \|v\|(0.5 + \varepsilon)^{1/2}$ cannot occur in the assumption and, consequently, it must hold that $u'_n v < -\|v\|(0.5 + \varepsilon)^{1/2}$, finally showing that (A.3) is true.

We next search still for a simpler lower bound for (A.3). Observe first that our three assumptions

$$(u'_n v)^2 > \|v\|^2(0.5 + \varepsilon), \quad \|u_n + v\| \leq 1, \quad u'_n v \geq -1,$$

imply that $-1 \leq u'_n v \leq 0$ and, consequently, that $\|v\| < (0.5 + \varepsilon)^{-1/2}$. We then claim that,

$$1 - \left\{1 + \|v\|^2 - \sqrt{2(1 + 2\varepsilon)}\|v\|\right\}^{1/2} \geq \|v\|(\sqrt{0.5 + \varepsilon} - \sqrt{0.5 - \varepsilon}).$$

This inequality is equivalent to

$$1 + \|v\|^2 - \sqrt{2(1 + 2\varepsilon)}\|v\| \leq \{1 - \|v\|(\sqrt{0.5 + \varepsilon} - \sqrt{0.5 - \varepsilon})\}^2, \quad (\text{A.4})$$

which is a quadratic in $\|v\|$ and can easily be verified to hold when $\|v\| < (0.5 + \varepsilon)^{-1/2}$. Consequently in the sub-case (I), we have for T_n the bound

$$T_n \geq \rho_n \|v\|^2 (\sqrt{0.5 + \varepsilon} - \sqrt{0.5 - \varepsilon})^2.$$

What remains, is tackling the case where $\|P_n v\|^2/\|v\|^2 > 0.5 + \varepsilon$ and $\|u_n + v\| > 1$. In this case it holds that

$$\| \|u_n + v\| - 1 \| \geq \sqrt{0.5 + \varepsilon} \|v\|.$$

To see this, we note that the inequality is equivalent to having

$$2y \geq (C - 1)x^2 + 2\sqrt{C}x,$$

when $C = 0.5 + \varepsilon$ and $x, y \in \mathbb{R}$ satisfy $y^2 > Cx^2$, $x \geq 0$, $2y > -x^2$ and $y \geq -1$.

Consequently, in the sub-case (II), we have the lower bound

$$T_n \geq \rho_n(0.5 + \varepsilon)\|v\|^2.$$

Combining now all three lower bounds with the choice $\varepsilon = 0.1$ and observing that $(\sqrt{0.6} - \sqrt{0.4})^2 < 0.6$ and that $\|A_n^{-1}\|_2^{-1} \|G_n^{-1/2}\|_2^{-1} \|m\|_2 \leq \|A_n G_n^{1/2} m\|_2$, we get the desired claim. \square

Assume now that $\lambda_n \rightarrow 0$. Our next result shows that, when n is large enough, the minimizer b_{n,λ_n} is increasingly restricted to a small neighbourhood of $b_{n,0}$. In the result we let \mathcal{A}_n denote the event that

$$\mathcal{A}_n := \{\alpha_n > 0.5\alpha, \Omega_n > 0.5\Omega, 1.5\rho > \rho_n > 0.5\rho, \rho_n - \psi_n > 0.5(\rho - \psi), \psi_n < 1.5\psi\}.$$

The convergences $M_n \rightarrow_p M, G_n \rightarrow_p G$ then guarantee that $P(\mathcal{A}_n) \rightarrow 1$ as $n \rightarrow \infty$.

Lemma 3. Assume that $\lambda_n \rightarrow 0$. Fix $\varepsilon > 0$ and choose n_0 such that $\lambda_n \leq \varepsilon$ for all $n \geq n_0$. Then, for $n \geq n_0$, we have the implication,

$$\mathcal{A}_n \Rightarrow \left\{ \|b_{n,\lambda_n} - b_{n,0}\| \leq \frac{2\varepsilon\sqrt{p}}{C} \right\},$$

where C is a strictly positive constant depending only on $\rho, \psi, \Omega, \alpha$.

Proof of Lemma 3. In the notation of Lemma 2, under the event \mathcal{A}_n , we have that

$$\begin{aligned} & \min\{C_{1n}, C_{2n}\} \|A_n^{-1}\|_2^{-2} \|G_n^{-1/2}\|_2^{-2} \\ & \geq \min\left\{ \frac{0.2\rho(\rho - \psi)}{3\psi}, \frac{1}{2\rho} \right\} \frac{1}{18\rho^2} \Omega^2 \alpha \\ & =: C, \end{aligned}$$

where $C > 0$. Then, for $n \geq n_0$, if \mathcal{A}_n holds, we have, by Lemma 2,

$$\begin{aligned} & f_{n,\lambda_n}(a_{n,\lambda_n,m}^*, b_{n,0} + m) - f_{n,\lambda_n}(a_{n,\lambda_n,0}^*, b_{n,0}) \\ & \geq \|m\|_2 (C\|m\|_2 - \varepsilon\sqrt{p}). \end{aligned}$$

Now this implies that any candidate minimizer $b_{n,0} + m$ of Version I must have $\|m\|_2 < (2\varepsilon\sqrt{p})/C$. This is because, if $\|m\|_2 \geq (2\varepsilon\sqrt{p})/C$, we have

$$f_{n,\lambda_n}(a_{n,\lambda_n,m}^*, b_{n,0} + m) - f_{n,\lambda_n}(a_{n,\lambda_n,0}^*, b_{n,0}) \geq \frac{2\varepsilon^2 p}{C} > 0,$$

showing that any such $b_{n,0} + m$ cannot be a minimizer of the objective function of Version I. Thus the result is proven. \square

The consistency $b_{n,\lambda_n} - b_{n,0} \rightarrow_p 0$ now follows directly from Lemma 3 and the earlier fact that $P(\mathcal{A}_n) \rightarrow 1$ as $n \rightarrow \infty$.

Corollary 2. Assume that $\lambda_n \rightarrow 0$. Then we have,

$$\|b_{n,\lambda_n} - b_{n,0}\| = o_p(1),$$

as $n \rightarrow \infty$.

Let now $a_n, \lambda_n \rightarrow 0$ be such that $\lambda_n/a_n \rightarrow 0$. Applying Lemma 3 to such a sequence λ_n and with the choice $\varepsilon = \delta a_n$, for $\delta > 0$, yields the following stronger result

Corollary 3. Assume that $a_n, \lambda_n \rightarrow 0$ be such that $\lambda_n/a_n \rightarrow 0$. Then we have,

$$a_n^{-1} \|b_{n,\lambda_n} - b_{n,0}\| = o_p(1),$$

as $n \rightarrow \infty$.

For the next result, we make the assumption that G_n, M_n are scatter matrices. That is, they are a functions $G_n \equiv G_n(x_1, \dots, x_n)$, $M_n \equiv M_n(x_1, \dots, x_n)$ of a data set x_1, \dots, x_n and obey the transformation rules (affine equivariance)

$$\begin{aligned} G_n(Ax_1, \dots, Ax_n) &= A G_n(x_1, \dots, x_n) A', \\ M_n(Ax_1, \dots, Ax_n) &= A M_n(x_1, \dots, x_n) A', \end{aligned}$$

for any invertible $A \in \mathbb{R}^{p \times p}$.

Lemma 4. Assume that $c_n(G_n - G) = O_p(1)$ and that $c_n(M_n - M) = O_p(1)$ for some increasing sequence c_n . Then,

$$c_n \|a_{n,0} - \alpha\|_2 = O_p(1) \quad \text{and} \quad c_n \|b_{n,0} - \beta\|_2 = O_p(1).$$

Proof of Lemma 4. By the affine equivariance of G, M , the solution vector $b_{n,0}$ of Version II transforms as $b_{n,0} \mapsto (A^{-1})'b_{n,0}$ under the transformation $(x_1, \dots, x_n) \mapsto (Ax_1, \dots, Ax_n)$ [45]. The equivalent also holds for the solution vector of Version III. Now, as

$$\|b_{n,0} - \beta\|_2 \leq \|A'\|_2 \|(A^{-1})'b_{n,0} - (A^{-1})'\beta\|_2,$$

where $\|\cdot\|_2$ for a matrix argument denotes the spectral norm, the result $\|b_{n,0} - \beta\|_2 = \mathcal{O}_p(1/c_n)$ follows once we show that $\|(A^{-1})'b_{n,0} - (A^{-1})'\beta\|_2 = \mathcal{O}_p(1/c_n)$ for any single choice of A .

Choose then $A = O'G^{-1/2}$ where O is any orthogonal matrix containing the eigenvectors of $G^{-1/2}MG^{-1/2}$ as its columns. Calling the diagonal matrix of respective eigenvalues Λ , we thus have $AGA' = I_p$ and $AMA' = \Lambda$. Consequently, we may in the following assume that $G = I_p$ and that M is diagonal with strictly positive diagonal elements.

Let next u_n be the leading eigenvector of the matrix $G_n^{-1/2}M_nG_n^{-1/2}$ and let $u = e_1$ be the leading eigenvector of the matrix $G^{-1/2}MG^{-1/2}$. Then, Lemma 2 and Corollary 1 in [46] imply that $u_{n1}^2 - 1 = \mathcal{O}_p(1/c_n^2)$ and that $u_{nj} = \mathcal{O}_p(1/c_n)$, since we have assumed that the leading eigenvalue of $G^{-1/2}MG^{-1/2}$ is unique. By writing,

$$\sqrt{1 + \mathcal{O}_p(1/c_n^2)} - 1 = \frac{\mathcal{O}_p(1/c_n^2)}{\sqrt{1 + \mathcal{O}_p(1/c_n^2)} + 1} = \mathcal{O}_p(1/c_n^2),$$

we obtain, correcting the sign of u_n if necessary, that $u_{n1} - 1 = \mathcal{O}_p(1/c_n^2)$ and, consequently, that

$$\|u_n - e_1\|_2 = \mathcal{O}_p\left(\frac{1}{c_n}\right).$$

By Corollary 1, we have $b_{n,0} = G_n^{-1/2}u_n$ and $\beta = e_1$. Arguing as in the proof of Lemma 1 in [46], we obtain $\|G_n^{-1/2} - I_p\|_2 = \mathcal{O}_p(1/c_n)$, finally giving us,

$$\begin{aligned} \|b_{n,0} - \beta\|_2 &\leq \|b_{n,0} - G_n^{-1/2}e_1\|_2 + \|G_n^{-1/2}e_1 - e_1\|_2 \\ &\leq \|G_n^{-1/2}\|_2 \|b_{n,0} - e_1\|_2 + \|G_n^{-1/2} - I_p\|_2 \\ &= \mathcal{O}_p(1/c_n). \end{aligned}$$

Move next back to the case of general G and M . Now, $a_{n,0} = G_n^{1/2}b_{n,0}$ and the convergence of $a_{n,0}$ then follows from the convergence of G_n and $b_{n,0}$ using the triangle inequality and similar arguments as before. \square

Combining Corollary 3 and Lemma 4 via the triangle inequality, we obtain the following main result of this section.

Theorem 5. *Assume that $c_n(G_n - G) = \mathcal{O}_p(1)$ and that $c_n(M_n - M) = \mathcal{O}_p(1)$ for some increasing sequence c_n . Let $a_n, \lambda_n \rightarrow 0$ be such that $\lambda_n/a_n \rightarrow 0$ and that $a_n c_n = \mathcal{O}(1)$. Then,*

$$c_n \|b_{n,\lambda_n} - \beta\|_2 = \mathcal{O}_p(1).$$

References

- [1] N. Abrahamsen, P. Rigollet, Sparse Gaussian ICA, arXiv preprint arXiv:1804.00408 (2018).
- [2] M. Babaie-Zadeh, C. Jutten, A. Mansour, Sparse ICA via cluster-wise PCA, *Neurocomputing* 69 (2006) 1458–1466.
- [3] S. H. Baloch, H. Krim, M. G. Genton, Robust independent component analysis, in: *IEEE/SP 13th Workshop on Statistical Signal Processing*, 2005, IEEE, pp. 61–64.
- [4] Z. Boukouvalas, Y. Levin-Schwartz, V. D. Calhoun, T. Adali, Sparsity and independence: Balancing two objectives in optimization for source separation with application to fMRI analysis, *Journal of the Franklin Institute* 355 (2018) 1873–1887.
- [5] J.-F. Cardoso, Source separation using higher order moments, in: *International Conference on Acoustics, Speech, and Signal Processing*, pp. 2109–2112 vol.4.
- [6] J.-F. Cardoso, A. Souloumiac, Blind beamforming for non-Gaussian signals, in: *IEE Proceedings F-Radar and Signal Processing*, volume 140, pp. 362–370.
- [7] A. Chatterjee, S. Lahiri, Strong consistency of lasso estimators, *Sankhya A* 73 (2011) 55–78.

- [8] P. Chen, H. Hung, O. Komori, S.-Y. Huang, S. Eguchi, Robust independent component analysis via minimum γ -divergence estimation, *IEEE Journal of Selected Topics in Signal Processing* 7 (2013) 614–624.
- [9] Y. Chen, L. Niu, R.-B. Chen, Q. He, Sparse-group independent component analysis with application to yield curves prediction, *Computational Statistics & Data Analysis* 133 (2019) 76–89.
- [10] Y. Deng, Group Sparsity in Regression and PCA, Ph.D. thesis, University of Michigan, 2019.
- [11] D. L. Donoho, P. J. Huber, The notion of breakdown point, *A festschrift for Erich L. Lehmann* 157184 (1983).
- [12] L. Dümbgen, K. Nordhausen, Approximating symmetrized estimators of scatter via balanced incomplete U-statistics, *Annals of the Institute of Statistical Mathematics* 76 (2024) 185–207.
- [13] L. Dümbgen, K. Nordhausen, H. Schuhmacher, New algorithms for m-estimation of multivariate scatter and location, *Journal of Multivariate Analysis* 144 (2016) 200–217.
- [14] L. Dümbgen, K. Nordhausen, H. Schuhmacher, fastM: Fast Computation of Multivariate M-Estimators, 2018. R package version 0.0-4.
- [15] L. Dümbgen, M. Pauly, T. Schweizer, M-functionals of multivariate scatter, *Statistics Surveys* 9 (2015) 32–105.
- [16] L. Dümbgen, D. E. Tyler, On the breakdown properties of some multivariate m-functionals, *Scandinavian Journal of Statistics* 32 (2005) 247–264.
- [17] W. Fu, K. Knight, Asymptotics for lasso-type estimators, *Annals of Statistics* 28 (2000) 1356–1378.
- [18] P. Georgiev, F. Theis, A. Cichocki, H. Bakardjian, Sparse component analysis: a new tool for data mining, *Data Mining in Biomedicine* (2007) 91–116.
- [19] M. Hallin, C. Mehta, R-estimation for asymmetric independent component analysis, *Journal of the American Statistical Association* 110 (2015) 218–232.
- [20] K. Harada, H. Fujisawa, Estimation of structural causal model via sparsely mixing independent component analysis, *arXiv preprint arXiv:2009.03077* (2020).
- [21] R. A. Horn, C. R. Johnson, *Matrix Analysis*, Cambridge University Press, Cambridge, second edition, 2013.
- [22] P. O. Hoyer, S. Shimizu, A. Hyvärinen, Y. Kano, A. J. Kerminen, New permutation algorithms for causal discovery using ica, in: *Independent Component Analysis and Blind Signal Separation: 6th International Conference, ICA 2006, Charleston, SC, USA, March 5-8, 2006. Proceedings* 6, Springer, pp. 115–122.
- [23] P. J. Huber, E. M. Ronchetti, *Robust Statistics*, John Wiley & Sons, 2011.
- [24] A. Hyvärinen, Fast and robust fixed-point algorithms for independent component analysis, *IEEE Transactions on Neural Networks* 10 (1999) 626–634.
- [25] A. Hyvärinen, J. Karhunen, E. Oja, *Independent Component Analysis*, Wiley, 2001.
- [26] A. Hyvärinen, K. Raju, Imposing sparsity on the mixing matrix in independent component analysis, *Neurocomputing* 49 (2002) 151–162.
- [27] P. Ilmonen, J. Nevalainen, H. Oja, Characteristics of multivariate distributions and the invariant coordinate system, *Statistics & Probability letters* 80 (2010) 1844–1853.
- [28] P. Ilmonen, D. Paindaveine, Semiparametrically efficient inference based on signed ranks in symmetric independent component models, *The Annals of Statistics* (2011) 2448–2476.
- [29] L. Li, Sparse sufficient dimension reduction, *Biometrika* 94 (2007) 603–613.
- [30] D. Malioutov, M. Cetin, A. S. Willsky, A sparse signal reconstruction perspective for source localization with sensor arrays, *IEEE Transactions on Signal Processing* 53 (2005) 3010–3022.
- [31] R. A. Maronna, Robust m-estimators of multivariate location and scatter, *The annals of statistics* (1976) 51–67.
- [32] J. Miettinen, S. Taskinen, K. Nordhausen, H. Oja, Fourth moments and independent component analysis, *Statistical Science* 30 (2015) 372–390.
- [33] I. Ng, Y. Zheng, X. Dong, K. Zhang, On the identifiability of sparse ICA without assuming non-gaussianity, *Advances in Neural Information Processing Systems* 36 (2023) 47960–47990.
- [34] K. Nordhausen, H. Oja, Independent component analysis: A statistical perspective, *Wiley Interdisciplinary Reviews: Computational Statistics* 10 (2018) e1440.
- [35] K. Nordhausen, H. Oja, E. Ollila, Robust independent component analysis based on two scatter matrices, *Austrian Journal of Statistics* 37 (2008) 91–100.
- [36] K. Nordhausen, S. Sirkia, H. Oja, D. E. Tyler, ICSNP: Tools for Multivariate Nonparametrics, 2018. R package version 1.1-1.
- [37] H. Oja, S. Sirkia, J. Eriksson, Scatter matrices and independent component analysis, *Austrian Journal of Statistics* 35 (2006) 175–189.
- [38] F. Palsson, M. O. Ulfarsson, J. R. Sveinsson, Sparse Gaussian noisy independent component analysis, in: *2014 IEEE International Conference on Acoustics, Speech and Signal Processing (ICASSP)*, IEEE, pp. 4224–4228.
- [39] J. Pearl, *Causality*, Cambridge University Press, 2009.
- [40] S. Shimizu, P. O. Hoyer, A. Hyvärinen, A. Kerminen, M. Jordan, A linear non-Gaussian acyclic model for causal discovery, *Journal of Machine Learning Research* 7 (2006).
- [41] S. Sirkia, S. Taskinen, H. Oja, Symmetrised M-estimators of multivariate scatter, *Journal of Multivariate Analysis* 98 (2007) 1611–1629.
- [42] S. Taskinen, S. Sirkia, H. Oja, Independent component analysis based on symmetrised scatter matrices, *Computational Statistics & Data Analysis* 51 (2007) 5103–5111.
- [43] D. E. Tyler, A distribution-free M-estimator of multivariate scatter, *Annals of Statistics* (1987) 234–251.
- [44] D. E. Tyler, Breakdown properties of the m-estimators of multivariate scatter, *arXiv preprint arXiv:1406.4904* (2014).
- [45] D. E. Tyler, F. Critchley, L. Dümbgen, H. Oja, Invariant co-ordinate selection, *Journal of the Royal Statistical Society: Series B (Statistical Methodology)* 71 (2009) 549–592.
- [46] J. Virta, K. Nordhausen, Determining the signal dimension in second order source separation, *Statistica Sinica* 31 (2021) 135–156.
- [47] K. Zhang, L.-W. Chan, ICA with sparse connections, in: *International Conference on Intelligent Data Engineering and Automated Learning*, Springer, pp. 530–537.
- [48] K. Zhang, H. Peng, L. Chan, A. Hyvärinen, ICA with sparse connections: Revisited, in: *Independent Component Analysis and Signal Separation: 8th International Conference, ICA 2009, Paraty, Brazil, March 15-18, 2009. Proceedings* 8, Springer, pp. 195–202.

- [49] H. Zou, T. Hastie, `elasticnet`: Elastic-Net for Sparse Estimation and Sparse PCA, 2020. R package version 1.3.
- [50] H. Zou, T. Hastie, R. Tibshirani, Sparse principal component analysis, *Journal of Computational and Graphical Statistics* 15 (2006) 265–286.